

Elsevier required licence: © 2020

This manuscript version is made available under the
CC-BY-NC-ND 4.0 license

<http://creativecommons.org/licenses/by-nc-nd/4.0/>

The definitive publisher version is available online at

[**https://doi.org/10.1016/j.biortech.2020.123481**](https://doi.org/10.1016/j.biortech.2020.123481)

**Removal pathways of benzofluoranthene in a constructed wetland amended with
metallic ions embedded carbon**

*Zizhang Guo¹, Yan Kang², Zhen Hu¹, Shuang Liang¹, Huijun Xie³, Huu Hao Ngo⁴,
Jian Zhang^{1,*}*

¹ Shandong Key Laboratory of Water Pollution Control and Resource Reuse, School of Environmental Science and Engineering, Shandong University, Qingdao 266237, China.

² College of Environment and Safety Engineering, Qingdao University of Science and Technology, Qingdao 266042, China.

³ Environmental Research Institute, Shandong University, Qingdao 266237, China.

⁴ School of Civil and Environmental Engineering, University of Technology Sydney, Broadway, NSW 2007, Australia.

*** Corresponding author:**

zhangjian00@sdu.edu.cn

Abstract

The limited adsorption capacity of the substrate and the concentration of dissolved oxygen in constructed wetlands (CWs) have inhibited their ability to efficiently remove polycyclic aromatic hydrocarbons (PAHs) from wastewater. Presently, biochar and activated carbon modified with Fe^{3+} and Mn^{4+} were used as effective sorbents in the removal of benzofluoranthene (BbFA), a typical PAH, in CW microcosms. The addition of **metallic ions embedded carbon** increased $\text{NO}_3\text{-N}$ accumulation by the reduction of Fe^{3+} and Mn^{4+} , which led to improved BbFA degradation. Additionally, plant adsorption in root and stem sections were observed separately. The abundance of PAH-degrading microbes in the rhizosphere substrate was higher with the **metallic ions embedded carbon** than control group. The Fe^{3+} , Mn^{4+} and $\text{NO}_3\text{-N}$ served as electron acceptors increased BbFA microbial degradation. The removal pathways of BbFA in the modified CWs were proposed which involved settlement in the substrate, plant absorption, and microbial degradation.

Keywords: constructed wetland, benzofluoranthene, removal pathway, activated carbon, biochar

1. Introduction

Polycyclic aromatic hydrocarbons (PAHs) are typical, persistent organic pollutants (POPs) with low water solubility, high lipophilicity, and chemical stability. They are chemicals that threaten human health and the environment through bioaccumulation and are considered to be mutagenic and potentially carcinogenic (Bao et al., 2020; Ozaki et al., 2015). At present, the methods for removing PAHs from water include physical (Lamichhane et al., 2016), chemical (Bocos et al., 2015), and biological techniques (Liu et al., 2017). Among them, the physical and chemical methods are costly and cause secondary pollution usually. Biological methods are common removal processes due to their low cost, fewer chemical and energy additions, and less complex metabolites through mineralization. Constructed wetlands (CWs) use the comprehensive ecological effects of plants, soils or other substrates, and microorganisms to effectively remove PAHs (Kang et al., 2019). They have key advantages such as a low capital investment, low operating costs, and beautiful ecological landscapes. Most of the research on the removal of PAHs with CWs has mainly focused on the uptake by plants and microbial degradation, ignoring the role of **substrate** adsorption and removal as well as the synergistic effects between the chemical, physical, and biological processes (i.e., plants, sorbent and microorganisms) (Qin et al., 2019; Zhao et al., 2018). In addition, there are two limiting factors in the process of removing PAHs from CWs: (1) the weak adsorption capacity of the substrate cannot provide sufficient support for microbial degradation; and (2) insufficient dissolved oxygen (DO) in the wetland system cannot create suitable conditions for PAH microbial degradation (He et al., 2017; Xie et al., 2018). The above problems have severely limited the removal efficiency of CW technology on PAHs. Therefore, it is of great practical significance to further improve the removal of

PAHs via CW technology.

The adsorption and retention of the soil or substrate is a key parameter for the CWs to enhance their treatment performance. Conventional substrate materials that are widely distributed, cheap and readily available, such as river sand, gravel, and limestone (Bezbaruah & Zhang, 2003; Matamoros et al., 2007; Tee et al., 2009), are practical choices for CW engineering, but their adsorption capacity is often very low. Clay minerals, such as loam, montmorillonite and bentonite, have been widely used to remove PAHs (De Rozari et al., 2018; Zhou et al., 2018). These materials have good adsorption performance but they are usually small in particle size and can easily cause wetland blockage. Carbonaceous materials include biochar and activated carbon, which have a high surface area and porous structure with surface chemical functional groups, and have been proven to have excellent adsorption capacity for organic contaminants. Zhou et al. reported that biochar addition to CWs enhanced conventional nitrogen and phosphorus pollutant removal (Zhou et al., 2017). Wirasnita et al. found that activated carbon-amended constructed wetlands (AC-CWs) showed efficient and sustainable removal of four phenolic endocrine-disrupting compounds (bisphenol A, bisphenol F, bisphenol S, and 4-tert-butylphenol) from wastewater (Wirasnita et al., 2018).

The design characteristics of a CW system provide an anoxic environment for the soil or substrate employed. However, it is difficult to ensure the DO required for microbial aerobic degradation of PAHs is only via atmospheric reoxygenation and plant oxygen secretion. Therefore, it is particularly important to strengthen the anaerobic degradation of PAHs in a CW, which directly affects the degradation efficiency of the entire system. However, the mechanism of anaerobic degradation of PAHs is complex. At present, little is known about the rate and mechanism of

anaerobic degradation of PAHs by microorganisms. Lovley et al. reported that PAHs could use nitrate, sulfate, iron ions, and manganese ions as electron acceptors under anaerobic conditions, which decompose into CO₂ by ring opening (Lovley et al., 1995). However, the secondary pollution of water bodies caused by the addition of nitrates and sulfates to CW systems is difficult to control in engineering applications. Manganese and iron metal ions are suitable choices as electron acceptors, and research on these ions extensive (Wu et al., 2019; Xie et al., 2018). Moreover, metal ions constitute a cyclic reaction in a CW, which improves the intracellular and external mass transfer efficiency of the microbial degradation of PAHs as well as enhances the removal of targeted pollutants (Han et al., 2017; Shuai & Jaffé, 2019).

Based on the current limitations of CWs for the removal of PAHs, an innovative method to enhance the removal of PAHs in CWs modified with **metallic ions embedded carbon** is proposed. In this study, benzofluoranthene (BbFA) was selected as a typical PAH to investigate the removal performance and degradation pathways of CWs. The aims of this research were to: (1) elucidate whether **metallic ions embedded carbon**, by incorporation of Fe³⁺ and Mn⁴⁺ into biochar and activated carbon, could enhance the performance of CWs in terms of the removal of BbFA and other common pollutants; (2) determine the fate and transport of BbFA in CWs; and (3) elucidate the involvement of a biological process under the proposed CW conditions.

2. Materials and methods

2.1 Chemicals and materials

The BbFA (99% purity) used in this experiment was purchased from Aladdin Reagent (Shanghai, China). All the samples were added to 1 ppm standard substitute (p-terphenyl-d14 and 2-fluorobiphenyl) during PAH extraction for pretreatment recovery

rate calculations. The standard substitute was obtained from ANPEL Laboratory Technologies (Shanghai) Inc. The internal standards injected into the sample extracts for the purposes of quantitation were obtained from ANPEL Laboratory Technologies (Shanghai) Inc. All solvents used, including dichloromethane and methanol, were HPLC grade. Ferric citrate, MnO_2 , KNO_3 , $(\text{NH}_4)_2\text{SO}_4$, and sucrose were of analytically pure.

2.2. Preparation and characterization of modified carbon materials

Coconut shell (CS) was washed by tap water to remove impurities and dirt and was then dried completely. The treated CS was heated to 500°C and maintained for 1 h in a muffle furnace under pure N_2 conditions. After cooling to room temperature, the carbonized materials were thoroughly washed and dried completely under room temperature. The produced samples are referred to as biochar. Activated carbon was produced by CO_2 activation at 800°C for 1 h. Afterwards, a certain amounts of BC and activated carbon were fully soaked in a saturated ferric citrate (FC) or manganese dioxide (MnO_2) solution at a given ratio (g FC or MnO_2 /g carbon; 0.05) and then dried at 105°C for 10 h. The mixed samples were heated to 300°C and maintained for 1 h in a muffle furnace under pure N_2 conditions. After cooling, washing and drying, the samples were used for later experiments. The pore structure characteristics of the carbon materials were determined by N_2 adsorption/desorption at 77 K after degassing at 200°C for 6 h using a surface area analyzer (Quantachrome Corporation, USA).

2.3 Laboratory-scale constructed wetland setup and operation

The CW units were set up under a translucent shelter in the laboratory at Shandong University in Jinan, China. A total with 14 CW microcosms with a height of 70 cm and inner diameter of 25 cm (material: polyvinyl chloride) were designed in a vertical

subsurface flow style. A perforated PVC pipe was placed in the center of the system to measure DO. Washed gravel (3–5 cm in diameter) was placed in the bottom layer to a height of 5 cm. The main substrate consisted of washed quartz grains (5–10 mm) to a height of 60 cm, which varied for different CW systems. Different washed biochar and activated carbon (grain size 0-1.5 cm) materials were mixed in the quartz layer at a mass ratio of 1:4. The 14 CW units were divided into 7 groups consisting of two pairs; units were named as follows: (1) Control (filled only with quartz); (2) BC (filled with biochar); (3) BM (filled with manganese-modified biochar); (4) BF (filled with iron-modified biochar); (5) AC (filled with activated carbon); (6) AM (filled with manganese-modified activated carbon); and (7) AF (filled with iron-modified activated carbon). *Acorus calamus* was selected as the submerged macrophyte planted in CWs with an initial density of 8 plants per unit. **After planting on March 12, 2019, the plants were cultivated using microelements and Hoagland solution for one month.**

After acclimation of the cultivated plants and microorganisms, synthetic wastewater diluted with tap water was added to the top of the CW microcosms **from May 2019**. The wastewater contained sucrose, KNO_3 , $(\text{NH}_4)_2\text{SO}_4$, KH_2PO_4 , BbFA and other microelements based on the Class I (B) level according to the Wastewater Discharge Standard (GB 18918-2002). A solution of BbFA (1 g) dissolved in dichloromethane (1000 mL) was prepared. During the operational period, 5.4 mL BbFA solution (1000 ppm) was added to 180 L synthetic wastewater. The final concentration of BbFA in the wastewater was 0.03 mg/L. A sequential batch experimental model was adopted with a hydraulic retention time (HRT) of 3 days. **After stable for ten cycles, the experimental data was steady from June 2019 to November 2019.**

2.4 Sampling and analysis

2.4.1 Water sampling and analysis

Influent and effluent wastewater was collected before and after each cycle. The DO concentration was determined using an instrument (HQ40d, Hach, USA). After filtration through 0.45 μm cellulose acetate membranes, the concentrations of ammonium ($\text{NH}_4^+\text{-N}$), $\text{NO}_3^-\text{-N}$, COD, total nitrogen (TN) and total phosphorus (TP) were determined according to standard methods (Federation & Association, 2005). The BbFA concentration was measured by solid-phase extraction after pretreatment. The BbFA in 1000 mL wastewater was extracted into 1 mL dichloromethane, and the concentration was measured by gas chromatography/mass spectrometry (GC/MS) using the internal standard method. The pretreatment and measuring methods are described in detail in our previous research (Kang et al., 2019).

2.4.2 Plant sampling and analysis

To determine the effect of biochar and activated carbon on wetland plants, the BbFA concentration in plants was analyzed. The plants were harvested at the end of the experimental period in November; roots and stems were collected separately. With respect to the stem, the plants were sampled uniformly along the height. Plant samples were cut into pieces and freeze dried at -60°C for 72 h, after which the BbFA in 10 g plant samples was extracted into 20 mL of dichloromethane and methanol at a volume ratio of 1:1 using an accelerated solvent extraction. The extraction methods were based on the literature and standard methods (Chen et al., 2016). After extraction, the solution was filtered through a silica gel column (containing neutral chlorine dioxide, silica gel, and Na_2SO_4). The solution was concentrated to 1 mL by a vacuum concentrator (Vortex 600), the BbFA concentrations in roots and stems were

determined by GC/MS.

2.4.3 Substrate sampling and analysis

To determine substrate adsorption capacity and PAH settlement, the BbFA concentration along the depth profile of the substrate was analyzed. Four parts of the substrate, i.e., the substrate around roots and at 0–20 cm, 20–40 cm, and 40–60 cm depths, were collected separately using a five-point sampling method. Sieving was conducted to remove plant residues, and the substrate samples were mixed with quartz and carbon and then freeze dried for 72 h. The BbFA concentrations in the substrate were extracted into 20 mL dichloromethane and methanol according to a standard method (HJ 783-2016). The BbFA concentrations were determined by GC/MS according to U.S. Environmental Protection Agency (US EPA) 8270C. The inorganic nitrogen fractions in the substrate were extracted by 1 N KCl. After shock treatment for 2 h and centrifugation at 4000 rpm for 1 h, the NO₃-N contents in the supernatant were measured following US EPA method 352.1 (Stoliker et al., 2016).

2.4.4 Microbial abundance and community analysis

The microbes around the root and at 40–60 cm depth were further analyzed. Before extraction, 5 g dry substrate was mixed with 25 mL diluted water in a centrifuge. After ultrasound treatment for 1 h, the solution was filtered through a 0.22 μm cellulose acetate membrane. The DNA that adhered to the membrane was isolated using a MOBIO PowerSand™ DNA Isolation Kit (MoBio Laboratories, Inc., Carlsbad, CA, USA). Quantitative real-time PCR (qPCR) was conducted to characterize the microbial abundance of the bacterial 16S rRNA gene and nitrogen-related gene, (including *amoA*, *nrfA*, *nir*, *nosZ*, and *narG*, as well as the phosphorus-related genes (*PAOs*). In particular, the microbes involved in PAH degradation (PAH-

RHD_α) were analyzed using primer pair 610/911 (f/r). The qPCR reactions were performed following Li et al.'s methodology (Li et al., 2017). The microbial community was studied with Illumina high-throughput sequencing analysis conducted by Novogene Co., LTD. (Beijing, China). The V4-V5 region of the 16S rRNA genes was obtained. More details on the procedure can be found in the study published by Xie et al. (Xie et al., 2018).

2.5 Data analysis

All experimental data are expressed as the mean±standard deviation. ANOVA was conducted for statistical analyses using SPSS 13.0 software (SPSS Inc., Chicago, USA). The results were considered significant when the p value was less than 0.05.

3. Results and discussion

3.1 Performance of CW microcosms

The concentrations of the main pollutants in the effluent reached a steady state after stabilization. As shown in Fig. 1a and 1b, the TN concentration decreased to 7.11±0.69 and 5.20±0.49 mg/L in AC and BC, respectively, both of which showed higher TN removal efficiency than the control (11.57±2.08 mg/L) after 100 days. The results for BC were similar to those in another study (Zhou et al., 2017), but there is limited literature on CWs with activated carbon. The TN concentration in AM (6.65±0.75 mg/L) and AF (6.12±0.61 mg/L) were slightly lower than that in the AC group, and slightly higher concentrations were measured in the BM (6.25±0.61 mg/L) and BF (6.01±0.69 mg/L) groups than in the BC group ($p>0.05$). The TN concentration was strongly related to the NO₃⁻-N and NH₄⁺-N concentrations. The average effluent concentrations of NO₃⁻-N were higher than 9.81 mg/L in the control

group, especially under a cold temperature in the later period. BC had a slightly higher removal efficiency of NO_3^- -N ($80.9 \pm 2.00\%$) compared with AC ($76.4 \pm 2.99\%$). The NO_3^- -N concentrations in AM (4.43 ± 0.52 mg/L) and AF (4.06 ± 0.49 mg/L) were lower than that in AC (5.20 ± 0.57 mg/L), but there was little difference among BC (4.22 ± 0.34 mg/L), BM (4.13 ± 0.40 mg/L) and BF (3.96 ± 0.34 mg/L). Hence, Fe^{3+} and Mn^{4+} enhanced NO_3^- -N removal in the CWs when incorporated with activated carbon. The efficiency of NO_3^- -N removal was related to the DO and COD concentrations. The DO concentration in CWs with carbon decreased due to the increased organic carbon removal and oxygen consumption. In addition, the DO concentrations were further decreased in the metal-modified carbon materials, mainly due to the redox potential of Fe^{3+} and Mn^{4+} . The influent and effluent COD of the seven treatments showed little difference ($p > 0.05$), but the concentrations were consistently higher in the control group. Hence, the biochar and activated carbon played an important role in COD reduction due to the improved physicochemical properties of each material. The COD reduction was similar, the modification with Fe^{3+} and Mn^{4+} can enhance adsorption capacity. NH_4^+ -N removal in BM ($87.0 \pm 2.11\%$) and BF ($89.6 \pm 2.13\%$) was slightly lower than that in BC ($94.2 \pm 1.78\%$) due to the DO limitation. As described by Zhou et al. (Zhou et al., 2017) and El-Naas et al. (El-Naas et al., 2010), both activated carbon and biochar play important roles in pollutant removal due to higher adsorption. The CWs with activated carbon addition showed slightly lower NH_4^+ -N removal efficiency compared with the control ($89.5 \pm 1.78\%$) and CWs with biochar.

Phosphorus is another important water quality indicator in CWs. Generally, the effluent phosphorus concentration in CWs with biochar was lower than that with activated carbon (Fig. 1). Furthermore, the AC (0.35 ± 0.09 mg/L) and BC (0.21 ± 0.03 mg/L) groups had higher TP effluent than the control (0.14 ± 0.02 mg/L). These results

are similar to those presented by Yao et al. (Yao et al., 2011). However, the biochar and activated carbon modified with Fe^{3+} improved phosphorus removal in the CWs. Previous studies have shown that the Fe^{2+} produced by Fe^{3+} reduction in anaerobic aquatic sediments had a positive effect on phosphorus removal because phosphorus can be precipitated in the form of iron phosphate and then be further adsorbed and removed (Ju et al., 2014).

Fig. 2 shows the concentration of BbFA with its removal efficiency over time for all the CWs tested in this study. The removal of BbFA in the CWs with biochar exceeded 99%, i.e., higher than the control (83%). Further, BbFA removal in the CWs with activated carbon exceeded 99%. The results indicated that both biochar and activated carbon contributed to the removal of BbFA, which could be attributed to enhanced PAH biodegradation (Kong et al., 2018). There was no difference between biochar and activated carbon compared to the modified carbons with Fe^{3+} and Mn^{4+} . It is well known that the surface area and pore volume, as well as interactions such as Van der Waals forces, hydrogen-bonding interactions, and π - π EDA values of biochar and activated carbon, can improve organic contaminant removal from wastewater (Yang et al., 2018), even without further modifications to the material.

3.2 Performance of plant uptake in CWs.

Wetland plants have four potential mechanisms for PAH remediation: adsorption, volatilization, transformation by plant excretion, and removal by microbes in the rhizosphere (García-Sánchez et al., 2018). Among these mechanisms, adsorption and rhizodegradation are the main pathways for PAH removal (Qin et al., 2019). The BbFA concentration in plants and in roots are illustrated in Fig. 3. The concentrations of BbFA in roots were higher by an order of magnitude than those in the stem and leaf, reflecting that the BbFA taken up from the substrate by plants is mainly stored in

the belowground tissue. The results indicated that the wetland plants contributed to the adsorption of BbFA, and the roots had a much higher accumulation ability; this was caused by the exchange of BbFA among the overlying water, stem and leaf, and sediment as well as the lower mass of the root than the stem and leaf. The AM and BM groups had higher BbFA concentrations in the aboveground parts of the plant, which were 28.4% and 154% higher, respectively, than those in the AC and BC groups. The plants in CWs with Fe³⁺-modified biochar ($48.2 \pm 6.65 \mu\text{g/g}$) or activated carbon ($54.2 \pm 10.6 \mu\text{g/g}$) had higher BbFA concentrations in roots compared with BC ($43.6 \pm 3.31 \mu\text{g/g}$) and AC ($32.9 \pm 11.8 \mu\text{g/g}$) groups. Plant photosynthesis enhanced the Fe ion reduction-oxidation turnover process. BF and AF had lower BbFA concentrations in the stem and leaf compared with BC and AC. Iron is an important essential element involved in plant growth and metabolism (Schmidt, 2003). Furthermore, due to the immobilization of Fe-formed oxide precipitates and decreased solubility, translocation of pollutants from the root section to aboveground tissue was limited (Wu et al., 2019).

3.3 Removal efficiency of BbFA in the substrate

Due to the settling characteristics of PAHs, the concentrations of BbFA at different depths of the substrate (rhizosphere, 0–20 cm, 20–40 cm, and 40–60 cm depth) were studied and the results are presented in Fig. 4a. The BbFA concentration in the control ($1.14 \mu\text{g/g}$) was significantly higher at each depth compared with the six other treatments. The BbFA accumulated in the substrate in the CWs with biochar and activated carbon in the following order: BC ($0.16 \pm 0.04 \mu\text{g/g}$) > BM ($0.15 \pm 0.04 \mu\text{g/g}$) > BF ($0.14 \pm 0.02 \mu\text{g/g}$) > AC ($0.12 \pm 0.08 \mu\text{g/g}$) > AM ($0.11 \pm 0.05 \mu\text{g/g}$) > AF ($0.07 \pm 0.06 \mu\text{g/g}$). Compared with the CWs with biochar, the BbFA concentrations in CWs with activated carbon were lower, due to the larger specific surface area

provides sites for microbial degradation. Mn^{4+} and Fe^{3+} are important oxidants known to degrade and mineralize organic compounds efficiently (Dong et al., 2017). Indeed, the BbFA contents were relatively higher at 0–20 cm depth, with an average concentration of $0.40 \pm 0.15 \mu\text{g/g}$ in the control and $0.17 \pm 0.02 \mu\text{g/g}$ in the six other treatment groups. Similarly, the BbFA contents in the rhizosphere were $0.35 \pm 0.06 \mu\text{g/g}$ in the control and $0.15 \pm 0.04 \mu\text{g/g}$ in the rest of the treatments. This significant decrease can be related to the plaques formed by iron and manganese, which can enhance pollutant accumulation in plants and thus decrease the BbFA contents in the rhizosphere substrate (Zhu et al., 2018). The reduced valency of Fe^{2+} and Mn^{2+} would cause oxidation to Fe^{3+} and Mn^{4+} , respectively, in the rhizosphere environment, which could also precipitate organic pollutants. However, the control had high BbFA contents at 40–60 cm depth, i.e., $0.24 \pm 0.03 \mu\text{g/g}$, indicating that the BbFA in CWs with biochar and activated carbon could remain in the superficial substrate instead of undergoing precipitation in the deep layer. By contrast, it indicated that iron and manganese contributed to the removal of BbFA in the deep substrate, which was mainly due to the reduction environment and the anaerobic conditions, which provided electron acceptors for BbFA biodegradation.

Anaerobic biodegradation of PAHs is an important pathway in subsurface CWs that is highly dependent on electron receptors such as nitrate and metal oxides (Kümmel et al., 2016; Yu et al., 2017). As a significant factor for PAH removal, the concentrations of NO_3^- -N at different depths of the substrate were determined, as shown in Fig. 4b. The concentrations of NO_3^- -N in CWs with biochar and activated carbon were significantly higher, approximately 0.05 and 0.1 mg/g, respectively, than that in the control group (0.003 mg/g); this might be related to pollutant sedimentation and adsorption by biochar and activated carbon (Kasak et al., 2018). Compared with

the BC (0.048 mg/g) group, the contents of NO₃-N in the BM (0.053 mg/g) and BF (0.051 mg/g) groups were higher in the whole substrate. Similarly, AM (0.28 mg/g) and AF (0.16 mg/g) had higher NO₃-N contents in the substrate compared to AC (0.10 mg/g). Based on the particular oxygen level in the substrate, which showed an aerobic environment in the superficial substrate and an anaerobic environment in the deeper substrate, reduction of Fe and Mn occurred (Xie et al., 2018). The reduction of the metal ions promotes NO₃-N accumulation. For example, NH₄⁺-N can transform into NO₃-N and NO₂-N during the reduction of Fe³⁺ to Fe²⁺ (Wu et al., 2019). Compared to BM and AM, BF and AF had slightly lower NO₃-N accumulation in the substrate. This was mainly because Fe²⁺-dependent nitrate removal as an alternative denitrification process is spontaneous ($10\text{Fe}^{2+} + 2\text{NO}_3^- + 24\text{H}_2\text{O} \rightarrow 10\text{Fe}(\text{OH})_3 + \text{N}_2 + 18\text{H}^+$) (Wu et al., 2019). Among the four layers of the substrate, the rhizosphere substrate had higher NO₃-N accumulation due to the roots releasing oxygen, which limited denitrification. Subsequently, the content of NO₃-N at 20–40 and 40–60 cm depths was also higher, which indicated that adequate NO₃-N could be involved in the coupled digestion of BbFA during anaerobic microbial degradation.

The enhanced BbFA removal in the substrate with the proposed **metallic ions embedded carbon** based materials might be attributed to the following mechanisms: the improved adsorption capacity of biochar and activated carbon, as well as the well-development surface area and porosity; and increased NO₃-N accumulation provided by the reduction of Fe³⁺ and Mn⁴⁺ that led to improved BbFA degradation.

3.4 Microbial performance in CWs.

According to the different oxygen levels in the subsurface flow of CWs, diverse micro-environments existed and provided various conditions for pollutant removal.

The root exudates could stimulate microbial growth capable for PAH degradation. BbFA biodegradation was improved at 40–60 cm depth. In the rhizosphere substrate, microbes for nitrification (*amoA*) and denitrification (*nirS*, *nirK*, and *narG*) were increased in the treatments containing biochar and activated carbon, as well as in the Fe³⁺ and Mn⁴⁺ modified materials, compared with the control. However, the increase in the abundance of denitrifiers and PAOs in BM, BF, AM, and AF was slightly lower than that in BC and AC ($p>0.05$). This means that the increased removal efficiency of NO₃-N and phosphorus in CWs was mainly due to the carbon source, supplementation of electron acceptors, and precipitation of ions, instead of the role of Fe³⁺ and Mn⁴⁺ in functional genes. The *16S rRNA* abundance was slightly lower in the control, which indicated that the biochar and activated carbon increased the number of bacterial cells.

The Illumina high-throughput results for 16S rRNA gene sequencing data were used to evaluate the microbial community in rhizosphere substrate. The BC (1587±121) and AC (1721±2.8) had more microbial species than the control (1552±108). Modification with Fe³⁺ and Mn⁴⁺ decreased the number of microbial species. The microbial richness and diversity indexes showed no difference among all CWs. The total operational taxonomic units (OTU) numbers were highest in BC (63250±1907), followed by AC (62890±1959), AM (62476±626), AF (58810±1688), BM (62318±3347), and BF (59349±2588), and were higher than that in the control (53740±4239). The porosity of activated carbon and biochar provided a habitat for interactions between pollutants and microbes. However, Fe³⁺ and Mn⁴⁺ occupied adsorption sites and decreased porosity, resulting in fewer sites for microbial presence. *Proteobacteria* and *Actinobacteria* at the phylum level in each CW were predominant in all CWs. The CWs with biochar and activated carbon had a higher

proportion of *Proteobacteria* than the control group; these materials played an important role in NO₃-N removal (Jia et al., 2020).

Researchers have reported several microorganisms with the potential to biodegrade PAH including the *Proteobacteria* (e.g., *Acinetobacter*, *Pseudomonas*, *Pseudoxanthomonas*, *Methylophilaceae*, *Methylobacillus*, *Comamonas*, *Nitrosomonas*, *Xanthomonas*, *Achromobacter*, *Sphingomonas*), *Actinobacteria* (e.g., *Nocardioideis*, *Arthrobacter*, *Mycobacterium*, *Rhodococcus*), *Firmicutes* (e.g., *Bacillus*, *Paenibacillus*, *Staphylococcus*), *Bacteroidetes* (e.g., *Chryseobacterium*, *Flavobacterium*) and *Cyanobacteria* (e.g., *Cyanobacteria*) (Ahmad et al., 2019; Gao et al., 2006; Li et al., 2018; Lladó et al., 2015; Sun et al., 2019; Yuan et al., 2017).

The diversity and relative abundance of PAH-degrading microbes in the rhizosphere substrate in different groups are shown in Fig. 5. The total relative abundance of PAH degrading bacteria was higher with the CWs containing the activated carbon substrate compared to the control. AC, AF and AF have 7.5%, 9.0% and 20.5% relative abundance, respectively, compared to 7.0% for the control. This result coincides with the BbFA concentrations in the substrate (Fig. 4a), reflecting that the effect of activated carbon on microbes is attributed to high BbFA removal. Among the microbes, the relative abundance of *Cyanobacteria* was higher in AM (14.0%).

Cyanobacteria can break down PAHs and provide electron acceptors for pollutants, similar to other photosynthetic bacteria (Subashchandrabose et al., 2011).

Cyanobacteria may coexist with manganese-oxidizing bacteria in AM (Hawco & Saito, 2018). Compared to the CWs with activated carbon, the BC (7.1%), BM (6.1%) and BF (6.3%) groups exhibited a lower relative abundance of PAH-degrading bacteria. Despite that the PAH-degrading bacteria had a lower relative abundance in BM and BF than in the control, the absolute abundance of these bacteria was still

higher in these two groups.

3.5 Proposed mechanisms of BbFA removal in CWs

Fig. 6 illustrates the potential degradation pathways of BbFA in CWs with biochar and activated carbon-based materials. The BbFA from the influent can undergo four main pathways: final water flow, settlement in the substrate, plant absorption and microbial degradation. Under aerobic conditions of the upper substrate, the oxidation-reduction reactions of Fe^{3+} and Mn^{4+} promoted BbFA removal. The porosity of biochar and activated carbon could also adsorb BbFA and provide a habitat for microbes, thus enhancing the microbial degradation of BbFA. Under anaerobic conditions, anaerobic microbial degradation also played a major role in BbFA removal. Fe^{3+} and Mn^{4+} increased the $\text{NO}_3\text{-N}$ contents in the deeper substrate and altered the microbial community toward BbFA degradation. Fe^{3+} , Mn^{4+} and $\text{NO}_3\text{-N}$ served as electron acceptors for BbFA microbial degradation.

4. Conclusions

In this study, enhanced removal of BbFA and other pollutants in CWs was obtained via improved adsorption capacity of the substrate and higher abundance of microorganisms for biodegradation using **metallic ions embedded carbon**. The addition of Fe^{3+} - and Mn^{4+} -modified biochar and activated carbon increased $\text{NO}_3\text{-N}$ accumulation by the reduction of Fe^{3+} and Mn^{4+} , provided electric acceptors for improving microbial degradation of BbFA in substrate.

Acknowledgements

This work was supported by National Natural Science Foundation of China (No. 51908326 and 51720105013), China Postdoctoral Science Foundation (No. 2018M640632), and Major Innovation Project of Shandong Province (No.

2019JZZY010411).

Supplementary data

N₂ adsorption/desorption isotherms, BET surface area and pore volume of carbons, characteristics of the influent in CWs (mg/L), profile and photo of experimental microcosms, DO concentration, COD concentration, NH₄⁺-N concentration and removal efficiency, top 10 Bacterial community composition in rhizosphere at phylum level, qPCR analysis results, The observed species, Shannon, Simpson, Chao1, and ACE values in each microcosm can be found in e-version of this paper online.

References

- [1] Ahmad, M., Yang, Q., Zhang, Y., Ling, J., Sajjad, W., Qi, S., Zhou, W., Zhang, Y., Lin, X., Zhang, Y., 2019. The distinct response of phenanthrene enriched bacterial consortia to different PAHs and their degradation potential: a mangrove sediment microcosm study. *J. Hazard. Mater.* 380, 120863.
- [2] Bao, K., Zaccone, C., Tao, Y., Wang, J., Shen, J., Zhang, Y., 2020. Source apportionment of priority PAHs in 11 lake sediment cores from Songnen Plain, Northeast China. *Water Res.* 168, 115158.
- [3] Bezbaruah, A.N., Zhang, T.C., 2003. Performance of a constructed wetland with a sulfur/limestone denitrification section for wastewater nitrogen removal. *Environ. Sci. Technol.* 37(8), 1690-1697.
- [4] Bocos, E., Fernández-Costas, C., Pazos, M., Sanromán, M.Á., 2015. Removal of PAHs and pesticides from polluted soils by enhanced electrokinetic-Fenton treatment. *Chemosphere*, 125, 168-174.
- [5] Chen, F., Tan, M., Ma, J., Zhang, S., Li, G., Qu, J., 2016. Efficient remediation of PAH-metal co-contaminated soil using microbial-plant combination: A greenhouse study. *J. Hazard. Mater.* 302, 250-261.
- [6] De Rozari, P., Greenway, M., El Hanandeh, A., 2018. Nitrogen removal from sewage and septage in constructed wetland mesocosms using sand media amended with biochar. *Ecol. Eng.* 111, 1-10.
- [7] Dong, C.-D., Chen, C.-W., Hung, C.-M. 2017., Synthesis of magnetic biochar from bamboo biomass to activate persulfate for the removal of polycyclic aromatic hydrocarbons in marine sediments. *Bioresource Technol.* 245, 188-195.
- [8] El-Naas, M.H., Al-Zuhair, S., Alhajja, M.A., 2010. Reduction of COD in refinery wastewater through adsorption on date-pit activated carbon. *J. Hazard. Mater.* 173(1-3), 750-757.
- [9] Federation, W.E., Association, A.P.H. 2005., Standard methods for the examination of water and wastewater. *American Public Health Association (APHA): Washington, DC, USA.*
- [10] Gao, Y., Yu, X., Wu, S., Cheung, K., Tam, N., Qian, P., Wong, M.H., 2006. Interactions of rice (*Oryza sativa* L.) and PAH-degrading bacteria (*Acinetobacter* sp.) on enhanced dissipation of spiked phenanthrene and pyrene in waterlogged soil. *Sci. Total Environ.* 372(1), 1-11.

- [11] García-Sánchez, M., Košnář, Z., Mercl, F., Aranda, E., Tlustoš, P., 2018. A comparative study to evaluate natural attenuation, mycoaugmentation, phytoremediation, and microbial-assisted phytoremediation strategies for the bioremediation of an aged PAH-polluted soil. *Ecotox. Environ. Safe.* 147, 165-174.
- [12] Han, J.-C., Zhang, F., Cheng, L., Mu, Y., Liu, D.-F., Li, W.-W., Yu, H.-Q. 2017., Rapid release of arsenite from roxarsone bioreduction by exoelectrogenic bacteria. *Environ. Sci. Tech. Let.* 4(8), 350-355.
- [13] Hawco, N.J., Saito, M.A. 2018., Competitive inhibition of cobalt uptake by zinc and manganese in a pacific *Prochlorococcus* strain: Insights into metal homeostasis in a streamlined oligotrophic cyanobacterium. *Limnol. Oceanogr.* 63(5), 2229-2249.
- [14] He, H., Duan, Z., Wang, Z., Yue, B. 2017., The removal efficiency of constructed wetlands filled with the zeolite-slag hybrid substrate for the rural landfill leachate treatment. *Environ. Sci. Pollut. R.* 24(21), 17547-17555.
- [15] Jia, L., Liu, H., Kong, Q., Li, M., Wu, S., Wu, H., 2020. Interactions of high-rate nitrate reduction and heavy metal mitigation in iron-carbon-based constructed wetlands for purifying contaminated groundwater. *Water Res.* 169, 115285.
- [16] Ju, X., Wu, S., Zhang, Y., Dong, R. 2014., Intensified nitrogen and phosphorus removal in a novel electrolysis-integrated tidal flow constructed wetland system. *Water Res.* 59, 37-45.
- [17] Kang, Y., Xie, H., Li, B., Zhang, J., Ngo, H.H., Guo, W., Guo, Z., Kong, Q., Liang, S., Liu, J., 2019. Performance of constructed wetlands and associated mechanisms of PAHs removal with mussels. *Chem. Eng. J.* 357, 280-287.
- [18] Kasak, K., Truu, J., Ostonen, I., Sarjas, J., Oopkaup, K., Paiste, P., Kõiv-Vainik, M., Mander, Ü., Truu, M., 2018. Biochar enhances plant growth and nutrient removal in horizontal subsurface flow constructed wetlands. *Sci. Total Environ.* 639, 67-74.
- [19] Kong, L., Gao, Y., Zhou, Q., Zhao, X., Sun, Z., 2018. Biochar accelerates PAHs biodegradation in petroleum-polluted soil by biostimulation strategy. *J. Hazard. Mater.* 343, 276-284.
- [20] Kümmel, S., Starke, R., Chen, G., Musat, F., Richnow, H.H., Vogt, C., 2016. Hydrogen isotope fractionation as a tool to identify aerobic and anaerobic PAH biodegradation. *Environ. Sci. Technol.* 50(6), 3091-3100.
- [21] Lamichhane, S., Krishna, K.B., Sarukkalige, R., 2016. Polycyclic aromatic hydrocarbons (PAHs) removal by sorption: a review. *Chemosphere*, 148, 336-353.
- [22] Li, J., Luo, C., Zhang, G., Zhang, D., 2018. Coupling magnetic-nanoparticle mediated isolation (MMI) and stable isotope probing (SIP) for identifying and isolating the active microbes involved in phenanthrene degradation in wastewater with higher resolution and accuracy. *Water Res.* 144, 226-234.
- [23] Li, J., Zhang, D., Song, M., Jiang, L., Wang, Y., Luo, C., Zhang, G., 2017. Novel bacteria capable of degrading phenanthrene in activated sludge revealed by stable-isotope probing coupled with high-throughput sequencing. *Biodegradation*, 28(5-6), 423-436.
- [24] Liu, S.-H., Zeng, G.-M., Niu, Q.-Y., Liu, Y., Zhou, L., Jiang, L.-H., Tan, X.-f., Xu, P., Zhang, C., Cheng, M., 2017. Bioremediation mechanisms of combined pollution of PAHs and heavy metals by bacteria and fungi: A mini review. *Bioresour. Technol.* 224, 25-33.
- [25] Lladó, S., Covino, S., Solanas, A., Petruccioli, M., D'annibale, A., Viñas, M., 2015.

- Pyrosequencing reveals the effect of mobilizing agents and lignocellulosic substrate amendment on microbial community composition in a real industrial PAH-polluted soil. *J. Hazard. Mater.* 283, 35-43.
- [26] Lovley, D.R., Coates, J.D., Woodward, J.C., Phillips, E.J.P., 1995. Benzene Oxidation Coupled to Sulfate Reduction. *Appl. Environ. Microb.* 61(3), 953-958.
- [27] Matamoros, V., Arias, C., Brix, H., Bayona, J.M., 2007. Removal of pharmaceuticals and personal care products (PPCPs) from urban wastewater in a pilot vertical flow constructed wetland and a sand filter. *Environ. Sci. Technol.* 41(23), 8171-8177.
- [28] Ozaki, N., Takamura, Y., Kojima, K., Kindaichi, T., 2015. Loading and removal of PAHs in a wastewater treatment plant in a separated sewer system. *Water Res.* 80, 337-345.
- [29] Qin, Z., Zhao, Z., Adam, A., Li, Y., Chen, D., Mela, S.M., Li, H., 2019. The dissipation and risk alleviation mechanism of PAHs and nitrogen in constructed wetlands: The role of submerged macrophytes and their biofilms-leaves. *Environ. Int.* 131, 104940.
- [30] Schmidt, W. 2003., Iron solutions: acquisition strategies and signaling pathways in plants. *Trends Plant Sci.* 8(4), 188-193.
- [31] Shuai, W., Jaffé, P.R., 2019. Anaerobic ammonium oxidation coupled to iron reduction in constructed wetland mesocosms. *Sci. Total Environ.* 648, 984-992.
- [32] Stoliker, D.L., Repert, D.A., Smith, R.L., Song, B., LeBlanc, D.R., McCobb, T.D., Conaway, C.H., Hyun, S.P., Koh, D.-C., Moon, H.S., 2016. Hydrologic controls on nitrogen cycling processes and functional gene abundance in sediments of a groundwater flow-through lake. *Environ. Sci. Technol.* 50(7), 3649-3657.
- [33] Subashchandrabose, S.R., Ramakrishnan, B., Megharaj, M., Venkateswarlu, K., Naidu, R., 2011. Consortia of cyanobacteria/microalgae and bacteria: biotechnological potential. *Biotechnol. Adv.* 29(6), 896-907.
- [34] Sun, S., Wang, Y., Zang, T., Wei, J., Wu, H., Wei, C., Qiu, G., Li, F., 2019. A biosurfactant-producing *Pseudomonas aeruginosa* S5 isolated from coking wastewater and its application for bioremediation of polycyclic aromatic hydrocarbons. *Bioresour. Technol.* 281, 421-428.
- [35] Tee, H., Seng, C., Noor, A.M., Lim, P., 2009. Performance comparison of constructed wetlands with gravel-and rice husk-based media for phenol and nitrogen removal. *Sci. Total Environ.* 407(11), 3563-3571.
- [36] Wirasnita, R., Mori, K., Toyama, T., 2018. Effect of activated carbon on removal of four phenolic endocrine-disrupting compounds, bisphenol A, bisphenol F, bisphenol S, and 4-tert-butylphenol in constructed wetlands. *Chemosphere*, 210, 717-725.
- [37] Wu, S., Vymazal, J., Brix, H., 2019. Critical review: biogeochemical networking of iron in constructed wetlands for wastewater treatment. *Environ. Sci. Technol.* 53(14), 7930-7944.
- [38] Xie, H., Yang, Y., Liu, J., Kang, Y., Zhang, J., Hu, Z., Liang, S., 2018. Enhanced triclosan and nutrient removal performance in vertical up-flow constructed wetlands with manganese oxides. *Water Res.* 143, 457-466.
- [39] Yang, K., Zhu, L., Yang, J., Lin, D., 2018. Adsorption and correlations of selected aromatic compounds on a KOH-activated carbon with large surface area. *Sci. Total Environ.* 618, 1677-1684.
- [40] Yao, Y., Gao, B., Inyang, M., Zimmerman, A.R., Cao, X., Pullammanappallil, P., Yang, L., 2011. Biochar derived from anaerobically digested sugar beet tailings:

- characterization and phosphate removal potential. *Bioresource Technol.* 102(10), 6273-6278.
- [41] Yu, B., Tian, J., Feng, L., 2017. Remediation of PAH polluted soils using a soil microbial fuel cell: influence of electrode interval and role of microbial community. *J. Hazard. Mater.* 336, 110-118.
- [42] Yuan, K., Chen, B., Qing, Q., Zou, S., Wang, X., Luan, T., 2017. Polycyclic aromatic hydrocarbons (PAHs) enrich their degrading genera and genes in human-impacted aquatic environments. *Environ. Pollut.* 230, 936-944.
- [43] Zhao, Z., Qin, Z., Zhang, D., Hussain, J., 2018. Dissipation characteristics of pyrene and ecological contribution of submerged macrophytes and their biofilms-leaves in constructed wetland. *Bioresource Technol.* 267, 158-166.
- [44] Zhou, X., Liang, C., Jia, L., Feng, L., Wang, R., Wu, H., 2018. An innovative biochar-amended substrate vertical flow constructed wetland for low C/N wastewater treatment: impact of influent strengths. *Bioresource Technol.* 247, 844-850.
- [45] Zhou, X., Wang, X., Zhang, H., Wu, H., 2017. Enhanced nitrogen removal of low C/N domestic wastewater using a biochar-amended aerated vertical flow constructed wetland. *Bioresource Technol.* 241, 269-275.
- [46] Zhu, Y., Du, X., Gao, C., Yu, Z., 2018. Adsorption behavior of inorganic and organic phosphate by iron manganese plaques on reed roots in wetlands. *Sustainability* 10(12), 4578.

Figure Captions

Fig. 1. The concentrations and removal efficiency (%) of TN (a, b), NO₃⁻-N (c, d) and TP (e, f) in each microcosm. The line represents the pollutant concentration and the bar represents the removal efficiency.

Fig. 2. The concentration and removal efficiency (%) of BbFA in each microcosm. The line represents the pollutant concentration and the bar represents the removal efficiency.

Fig. 3. Uptake of BbFA in roots and stem leaf sections of plants.

Fig. 4. BbFA (a) and NO₃⁻-N (b) concentrations along the depth of the substrate.

Fig. 5. Relative abundances of PAH degradation genera in the rhizosphere substrate.

Fig. 6. Conceptual model for the mechanism of pollutant removal in proposed CWs.

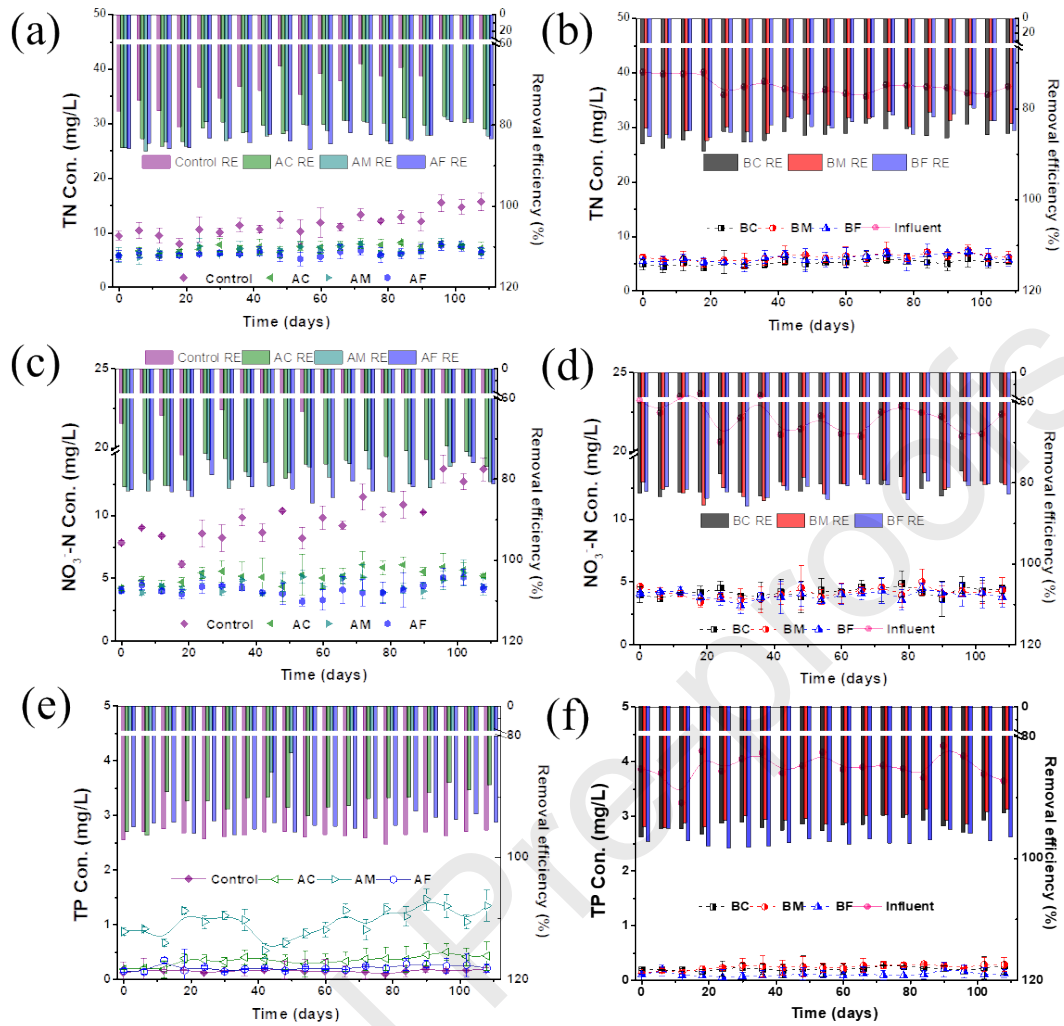


Fig. 1. The concentrations and removal efficiency (%) of TN (a, b), NO₃⁻-N (c, d) and TP (e, f) in each microcosm. The line represents the pollutant concentration and the bar represents the removal efficiency.

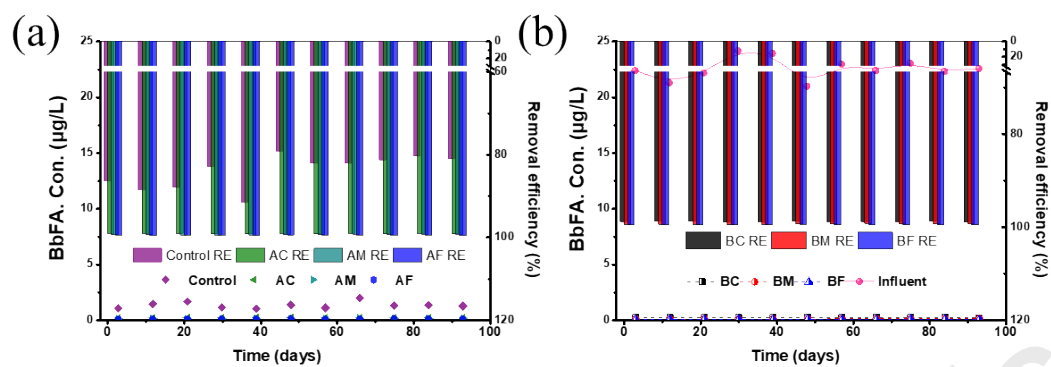


Fig. 2. The concentration and removal efficiency (%) of BbFA in each microcosm.

The line represents the pollutant concentration and the bar represents the removal efficiency.

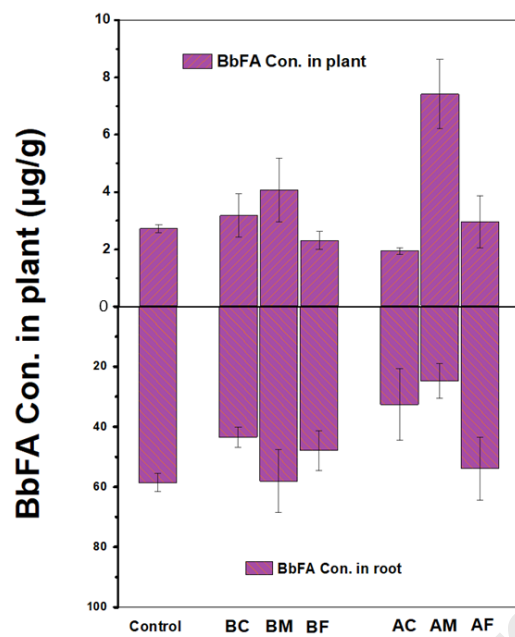


Fig. 3. Uptake of BbFA in roots and stem leaf sections of plants.

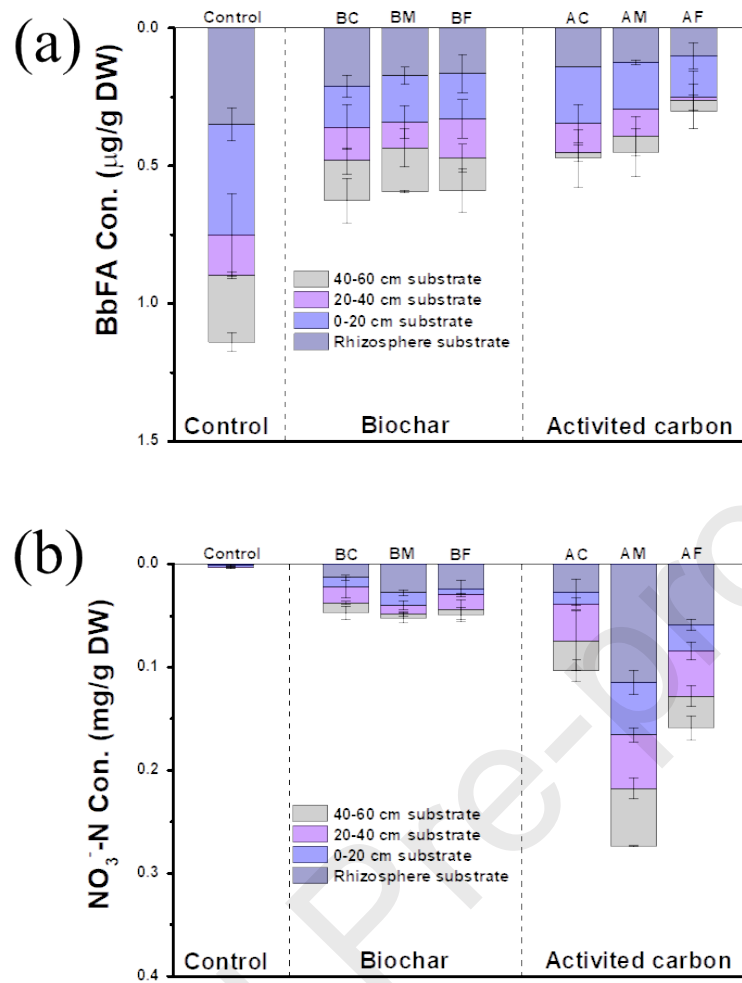


Fig. 4. BbFA (a) and NO_3^- -N (b) concentrations along the depth of the substrate.

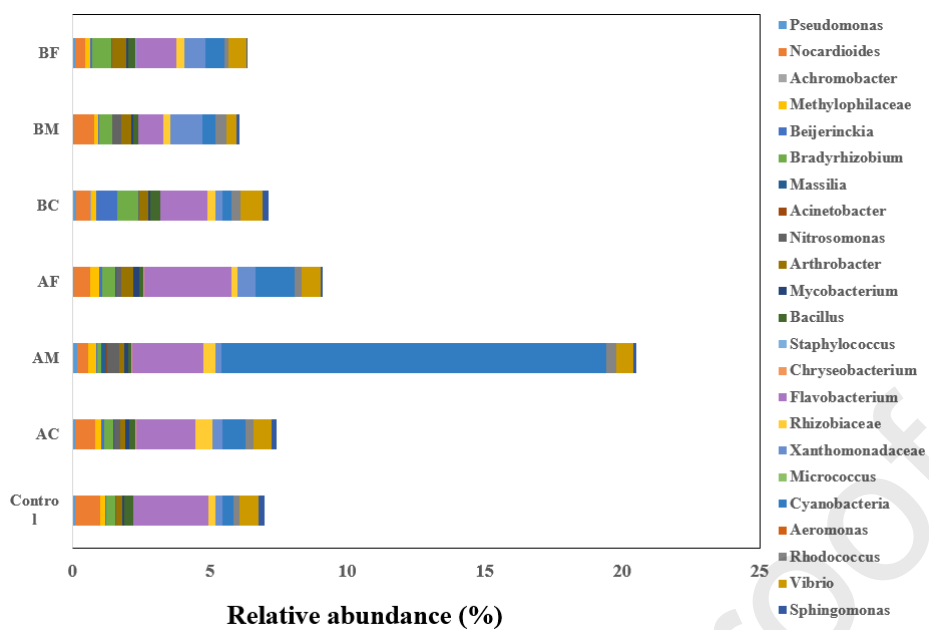


Fig. 5. Relative abundances of PAH degradation genera in the rhizosphere substrate.

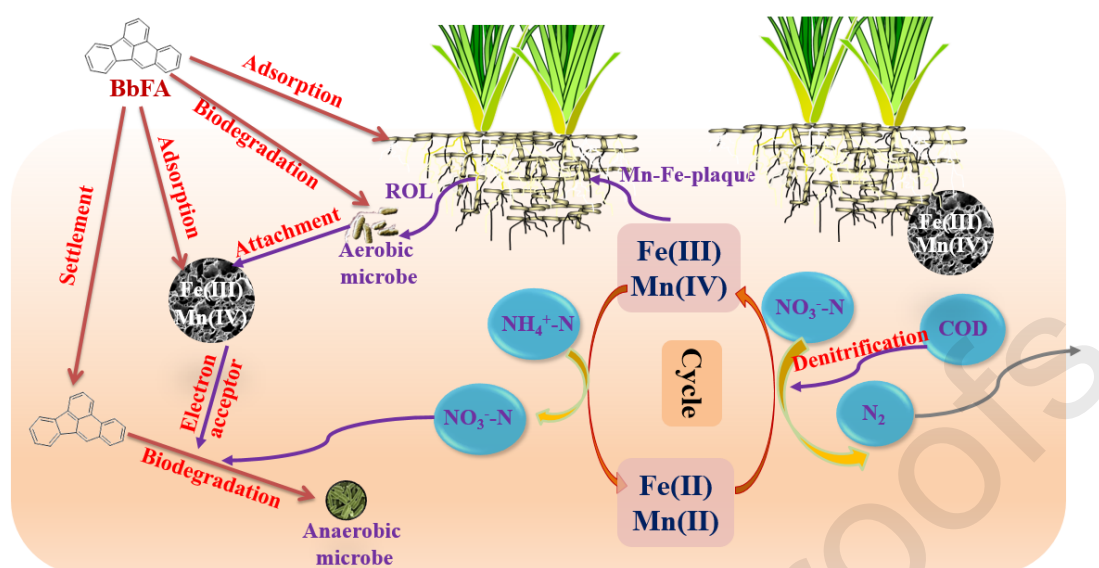


Fig. 6. Conceptual model for the mechanism of pollutant removal in proposed CWs.

Zizhang Guo: Conceptualization, Methodology, Writing - Review & Editing, Visualization, Funding acquisition. **Yan Kang:** Methodology, Formal analysis, Data Curation, Writing - Original Draft. **Zhen Hu:** Methodology. **Shuang Liang:** Funding acquisition. **Huijun Xie:** Methodology. **Huu Hao Ngo:** Project administration. **Jian Zhang:** Supervision, Project administration, Funding acquisition.

Declaration of interests

The authors declare that they have no known competing financial interests or personal relationships that could have appeared to influence the work reported in this paper.

The authors declare the following financial interests/personal relationships which may be considered as potential competing interests: